Hindawi Publishing Corporation
Advances in Materials Science and Engineering
Volume 2014, Article ID 189745, 10 pages
http://dx.doi.org/10.1155/2014/189745

Research Article

Molecular Simulation of Hydrogen Storage in Ion-Exchanged X Zeolites

Xiaoming Du

School of Materials Science and Engineering, Shenyang Ligong University, Shenyang 110159, China

Correspondence should be addressed to Xiaoming Du; du511@163.com

Received 5 May 2013; Revised 15 October 2013; Accepted 18 October 2013; Published 6 January 2014

Academic Editor: Jie Dai

Grand Canonical Monte Carlo (GCMC) method was employed to simulate the adsorption properties of molecular hydrogen on ion-exchanged X zeolites at 100–293 K and pressures up to 10 MPa in this paper. The effect of cation type, temperature, and pressure on hydrogen adsorption capacity, heat of adsorption, adsorption sites, and adsorption potential energy of ion-exchanged X zeolites was analyzed. The results indicate that the hydrogen adsorption capacity increases with the decrease in temperatures and the increase in pressures and decreases in the order of KX < LiX < CaX. The isosteric heat of adsorption for all the three zeolites decreases appreciably with the increase in hydrogen adsorption capacity. The hydrogen adsorption sites in the three zeolites were determined by the simulated distribution of hydrogen adsorption energy and the factors that influence their variations were discussed. Adsorption temperature has an important effect on the distribution of hydrogen molecules in zeolite pores.

1. Introduction

The utilization of hydrogen as a possible substitute for fossil fuels requires the solution of a number of problems related to hydrogen production, transportation, storage, and fuel cell technology [1]. Among them, safe and efficient storage of hydrogen is very important for hydrogen energy applications. Various methods for storing hydrogen were developed which include high-pressure tanks for gaseous hydrogen, cryogenic vessel for liquid hydrogen, and metal hydride for solid-state storage systems [2–4]. The first two methods bear the danger of explosion if handled improperly, and the latter one suffers high cost and weight. Recently, attention has been focused on light microporous materials such as carbon [5], aluminosilicate zeolites [6, 7], and metal organic frameworks (MOFs) [8] for storing hydrogen by adsorption because the adsorption is reversible and thus the sorbent can be recycled.

Zeolites are a large class of crystalline aluminosilicate materials that have high thermal stability and regular and single size pores and the diameter of the pores can be controlled by changing the size and charge of the exchangeable cations. Thus, they offer enormous potential for storage of gases. The hydrogen storage capacity of various types of zeolites had been reported experimentally and theoretically [9–12]. However, little attention was previously paid to the distribution of adsorption sites and adsorption potential energy for the molecular hydrogen on zeolites. Li and Yang [13] reported experimentally that the alkali-metal cations (Li^+, Na^+, K^+) and the framework atoms (Al, O, Si) in ion-exchanged X zeolites were the main adsorption sites of hydrogen. Kazansky et al. [14, 15] investigated the adsorption sites of hydrogen on ion-exchanged X and Y zeolites with various Si/Al ratios by using sorption and DRIFT spectra methods. The results indicated that the adsorbed hydrogen is located mainly at site II and site III inside the FAU zeolite supercages.

However, the studies on hydrogen storage in X type of zeolites are so far only limited to the conditions of the separate temperatures and low pressure owing to not being readily amenable to experiments. It is disadvantageous for our in-depth understanding of the mechanism of hydrogen storage in zeolites. Molecular simulation can provide a cost-effective way of determining adsorption isotherms and gives a useful insight into the adsorption behavior of molecular hydrogen inside zeolite channels and pores.

In this study, we performed the adsorption simulation of hydrogen on three alkali-metal and alkali-earth cations (Li^+, K^+, Ca^{2+}) exchanged X zeolites at the temperatures of

100–293 K and the pressures up to 10 MPa by using Grand Canonical Monte Carlo (GCMC) method. The dependence of the hydrogen adsorption capacity of zeolites on temperature, pressure, cation type, adsorption site distribution, and adsorption potential energy was discussed.

2. Computational Details

Structures of the initial unit cell of alkali-metal and alkali-earth metal cations (Li^+, K^+, Ca^{2+}) exchanged X zeolites such as LiX, KX, and CaX (X = $Si_{96}Al_{96}O_{384}$, Si/Al = 1.0) were constructed according to the results of X-ray crystallographic studies [16–18]. The crystal is cubic with unit cell parameters a = 25.099 Å and space group *Fd-3*. In dehydrated LiX zeolite, there are three Li^+ cation sites. 32 Li^+ cations are located in site I′ (in the β-cage, close to the hexagonal window to the hexagonal prism), site II (in the six-member ring of the β-cage), and site III (in the supercage, close to a square window between two other square windows), respectively. In dehydrated KX zeolite, there are four K^+ cation sites. The occupancies of these K^+ cations at cation sites I (in the hexagonal prism), I′, II, and III in zeolite KX are 16, 16, 32, and 32, respectively. For the dehydrated CaX zeolite, the Ca^{2+} cations are located in site I (12 Ca^{2+} cations), site I′ (4 Ca^{2+} cations), and site II (32 Ca^{2+} cations). After constructing the initial structure, we performed energy minimization calculations to determine the equilibrium structures using density function theory (DFT) method that was successfully used to explore hypothetical FAU with dense topologies [19]. DFT calculations were carried out with the code Quantum-ESPRESSO [20] which uses atom centered basis functions that are particularly efficient for total energy studies of very low density materials with very large unit cells. Periodic DFT calculations were carried out using the PBE exchange correlation functional within the GGA approximation. The zeolites with minimized energy were used as adsorbents for hydrogen adsorption.

For hydrogen adsorption on LiX, KX, and CaX zeolites, the force field used was an enhanced version of the polymer consistent force field (PCFF) [21]. Because the host of X zeolite was treated as a rigid structure, with fixed atom positions obtained from the minimized structure, at all simulations, the total energy of the zeolite framework and adsorbed molecules (E_{total}) is expressed as the sum of the short-range van der Waals (vdW) nonbond interaction energy (E_{vdW}) and the long-range coulombic interaction energy (E_{c}):

$$E_{\text{total}} = E_{\text{vdW}} + E_{\text{c}}. \tag{1}$$

The vdW interactions between hydrogen and the zeolite framework atoms are represented by Lennard-Jones (LJ) potential with the following expression:

$$E_{\text{vdW}} = \sum_i \sum_{j>i} \left(4\varepsilon_{ij} \left[\left(\frac{\sigma_{ij}}{r_{ij}} \right)^{12} - \left(\frac{\sigma_{ij}}{r_{ij}} \right)^{6} \right] \right), \tag{2}$$

where ε_{ij} and σ_{ij} are the LJ potential parameters that were obtained from ε_i and σ_i of each species by using the Lorentz Berthelot mixing rule (i.e., a geometric combining rule for the energy and an arithmetic one for the atomic size: $\varepsilon_{ij} = \sqrt{\varepsilon_i \cdot \varepsilon_j}$ and $\sigma_{ij} = (\sigma_i + \sigma_j)/2$). r_{ij} is the interatomic distance between the ith and jth atoms. The LJ potential parameters used in all simulations were summarized in Table 1.

Table 1: Lennard-Jones parameters used for hydrogen adsorption on ion-exchanged X zeolite.

Atom type	ε (kcal/mol)	σ (⊕)	Reference
H	0.0726	2.958	[22]
Si	0.0370	0.076	[23]
Al	0.0384	1.140	[23]
O	0.3342	3.040	[23]
Li	0.0249	2.180	[24]
K	0.0356	3.020	[24]
Ca	0.1553	2.980	[24]

The coulombic electrostatic interaction energy is the long-range interaction and the model systems are periodic. So Ewald sum was used for E_{c}:

$$E_{\text{c}} = \sum_i \sum_{j>i} \frac{q_i q_j}{r_{ij}}, \tag{3}$$

where q_i and q_j are the net atomic charges of the ith and jth atoms, respectively.

For the assignment of charges of extraframework cations Li^+, K^+, and Ca^{2+} and framework atoms Si, Al, and O, the values of charges were obtained by using the electronegativity equalization method (EEM), which are taken from the literature as given in Table 2 [25].

For hydrogen, we used three-point charge model [23, 26, 27], where the two outer sites are separated by a distance of l = 0.7414 Å having a charge of $q = -0.21e$ [28] and the third midpoint has a point charge of $-2q$.

All GCMC simulations were performed by employing the Multipurpose Simulation Code (MUSIC) [29]. The loading at a constant pressure and temperature was calculated by attempting, with equal probability, to insert, delete, or translate one H_2 molecule in the simulation cell. Trial moves considered here were the translation, insertion, and deletion of particles [30, 31]. The moves for each run were randomly chosen with equal probability. The random movements of molecules make new configurations, which may be accepted according to Metropolis's sampling scheme. Each structure model consists of one elementary cell with three-dimensional periodic boundary conditions. The cut-off distance for short-range LJ summation was set to 12 ⊕ which is less than half of the length of the simulation box (25.099 Å) and the half of the cell length for Ewald summation was used. The number of GCMC steps was set to 2×10^7 for each simulation. The number of trial moves in an MC cycle is equal to the number of adsorbed molecules. Usually, approximately 15% of the cycles were performed for equilibration, and the subsequent cycles were used for statistics. The simulation temperatures included 6 temperatures: 100 K, 140 K, 195 K, 230 K, 260 K, and 293 K.

Table 2: The atomic charges, q, for elements of the three zeolite models[a].

Zeolite	$q_{Si}(e)$	$q_{Al}(e)$	$q_{O(1)}(e)$	$q_{O(2)}(e)$	$q_{O(3)}(e)$	$q_{O(4)}(e)$	$q_{Li(I',II,III)}(e)$	$q_{K(I',II,III)}(e)$	$q_{Ca(I,I',II)}(e)$
LiX	1.26853	1.12745	−0.83069	−0.85591	−0.82155	−0.88782	1.0	—	—
KX	1.27615	1.13366	−0.87774	−0.84282	−0.79500	−0.89425	—	1.0	—
CaX	1.28523	1.13767	−0.74562	−1.00346	−0.88257	−0.79125	—	—	2.0

[a]In Li^+, K^+, and Ca^{2+} cations exchanged X zeolites, there are four oxygen sites O(1), O(2), O(3), and O(4).

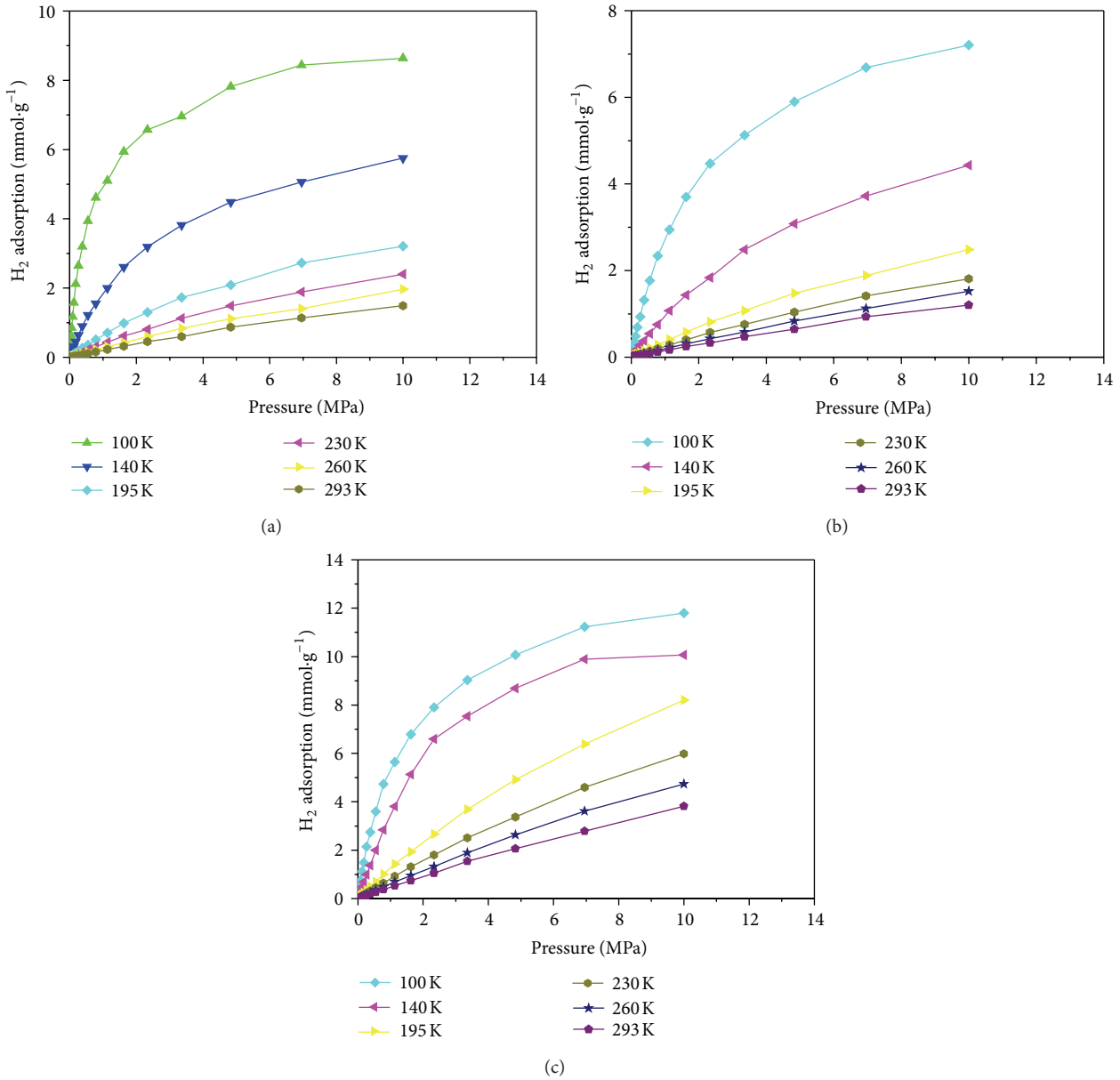

Figure 1: Calculated hydrogen adsorption isotherms for (a) LiX zeolite, (b) KX zeolite, and (c) CaX zeolite.

3. Results and Discussion

The hydrogen adsorption isotherms of LiX, KX, and CaX zeolites calculated at the temperatures of 100–293 K and the pressures up to 10 MPa with GCMC method were shown in Figure 1. All adsorption isotherms obtained under this study are Type I in nature, showing adsorption of hydrogen inside microporous zeolite cavities. As can be seen in Figure 1, the hydrogen adsorption capacity in terms of mmol/g decreases with increasing temperature within the simulation temperature range. The reason is that the hydrogen molecules have higher kinetic energy at higher temperature; thus, it is required for the larger adsorption potential energy to adsorb hydrogen molecules in zeolite cavities. The effect of pressure on hydrogen adsorption capacity has two-step characteristics. Namely, the hydrogen adsorption capacity rapidly increases

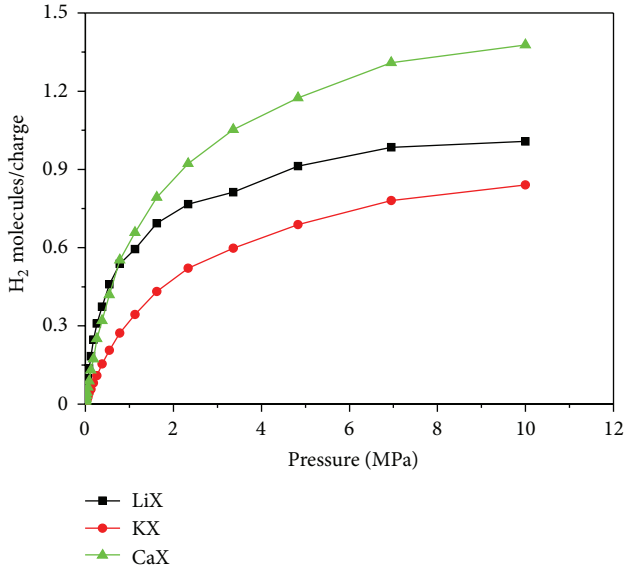

Figure 2: Number of adsorbed hydrogen molecules per cation charge as a function of pressure for LiX, KX, and CaX at 100 K.

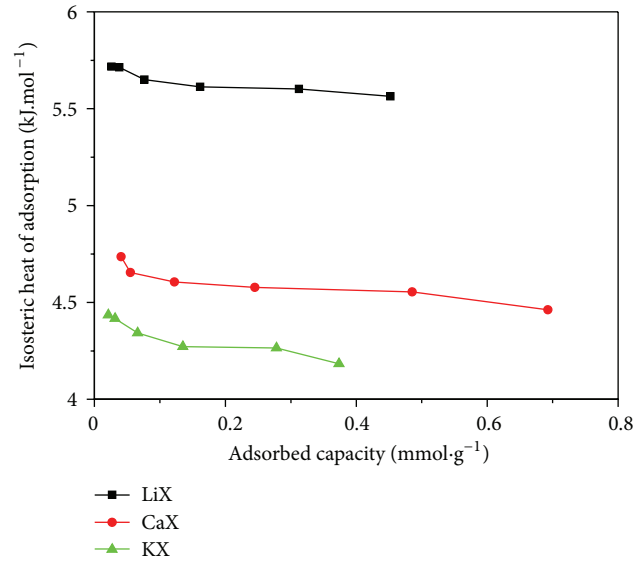

Figure 3: Relationship between isosteric heat of adsorption and adsorbed hydrogen on zeolites LiX, KX, and CaX.

with increasing pressure at low pressure (less than 1 MPa), whereafter it increases slowly at high pressure (above 4 MPa). The hydrogen adsorption capacity of the zeolites at any given pressure decreases in the order of CaX > LiX > KX and basically keeps the same order at all temperatures. The highest hydrogen adsorption capacity at 100 K and 10 MPa was obtained on zeolite CaX and calculated to be 2.31 wt.% through converting mmol/g value in Figure 1 to facilitate subsequent comparison with the literature data. The hydrogen adsorption capacities reported for LiX, KX, and CaX zeolites at above 100 K were very scarce in the literatures. Li and Yang [13] and Wang and Yang [32] reported that the hydrogen storage capacities on Li^+, Ca^{2+}, and Mg^{2+} ion-exchanged X type zeolites at 298 K and 10 MPa were 3 wt.%, 0.5 wt.%, and 0.27 wt.%, respectively. In this work, the calculated values of hydrogen storage capacity at 293 K and 10 MPa for LiX and CaX zeolites are 0.3 wt.% and 0.76 wt.%, respectively, as can be seen in Figure 1. There are two possible reasons for the aforementioned difference. Firstly, the unit cell structures used in simulation studies are perfect crystalline. However, the experimentally used Li^+, K^+ and Ca^{2+} cation exchanged zeolite samples are not always perfect crystalline. Cation exchange may result in partial breaking of the cages with the smaller window diameter, such as β-cage with six-member ring (about 2.6 ⊕). The hydrogen molecules can enter the cages. This could be the main reason for observance of higher hydrogen adsorption capacity from experimental results as compared with simulation calculations. However, preparation of such a sample is not practically feasible as zeolite samples lose crystallinity on cation exchange. Secondly, we used force field based simulation for the adsorption isotherm generation in which nonbonded interactions like van der Waals and coulombic interactions were considered. However, different parameterizations of the LJ potentials for the Al, Si, O, and metal cations of the zeolite X have been proposed in the literature on a theoretical basis, for instance, in [23, 24, 33]. They were used in simulation of gas adsorption, and sometimes were modified in order to achieve a better agreement between simulation and experimental results. In our simulations, the estimation of LJ parameters used for the simulation of hydrogen adsorption in the Li^+, K^+, and Ca^{2+} exchanged zeolites also has influence on the calculated hydrogen adsorption capacity.

In order to investigate the effect of cation exchange on the hydrogen adsorption, the curves of the number of hydrogen molecules per cation charge versus pressure at 100 K for Li^+, K^+ and Ca^{2+} exchanged X zeolites were simulated as shown in Figure 2. The profile of these curves is similar to that of the corresponding hydrogen adsorption isotherms shown in Figure 1. In the pressure range from 0 to 0.785 MPa, the number of hydrogen molecules per cation charge follows the order LiX > CaX > KX, whereas the order changes to CaX > LiX > KX in the pressure range from 0.785 to 10 MPa. As a result, a "crossover" of the hydrogen adsorption isotherm curves for CaX and LiX zeolites appears. This trend of hydrogen adsorption in these zeolites may be explained by Franekel's [34] earlier observations and postulation that hydrogen uptake in zeolites was related to the available void volume per gram of zeolite which decreases with increasing size and number of the exchangeable cations. The KX containing larger alkali-metal K^+ cations has the same number of exchangeable cations as that of LiX but occupy a substantially bigger space, with a consequent reduction in void volume available for hydrogen adsorption. However, when Na^+ cations in NaX are replaced by alkaline-earth metal divalent cations (i.e., Ca^{2+}), the number of cations in zeolite decreases; thus the available void volume increases accordingly. Hydrogen uptake had previously been shown to be related to the micropore volume in zeolites [7]. The available void volume is related to the number and size of exchangeable cations [34]. In general, zeolites containing alkali-metal and alkaline-earth metal cations have a large

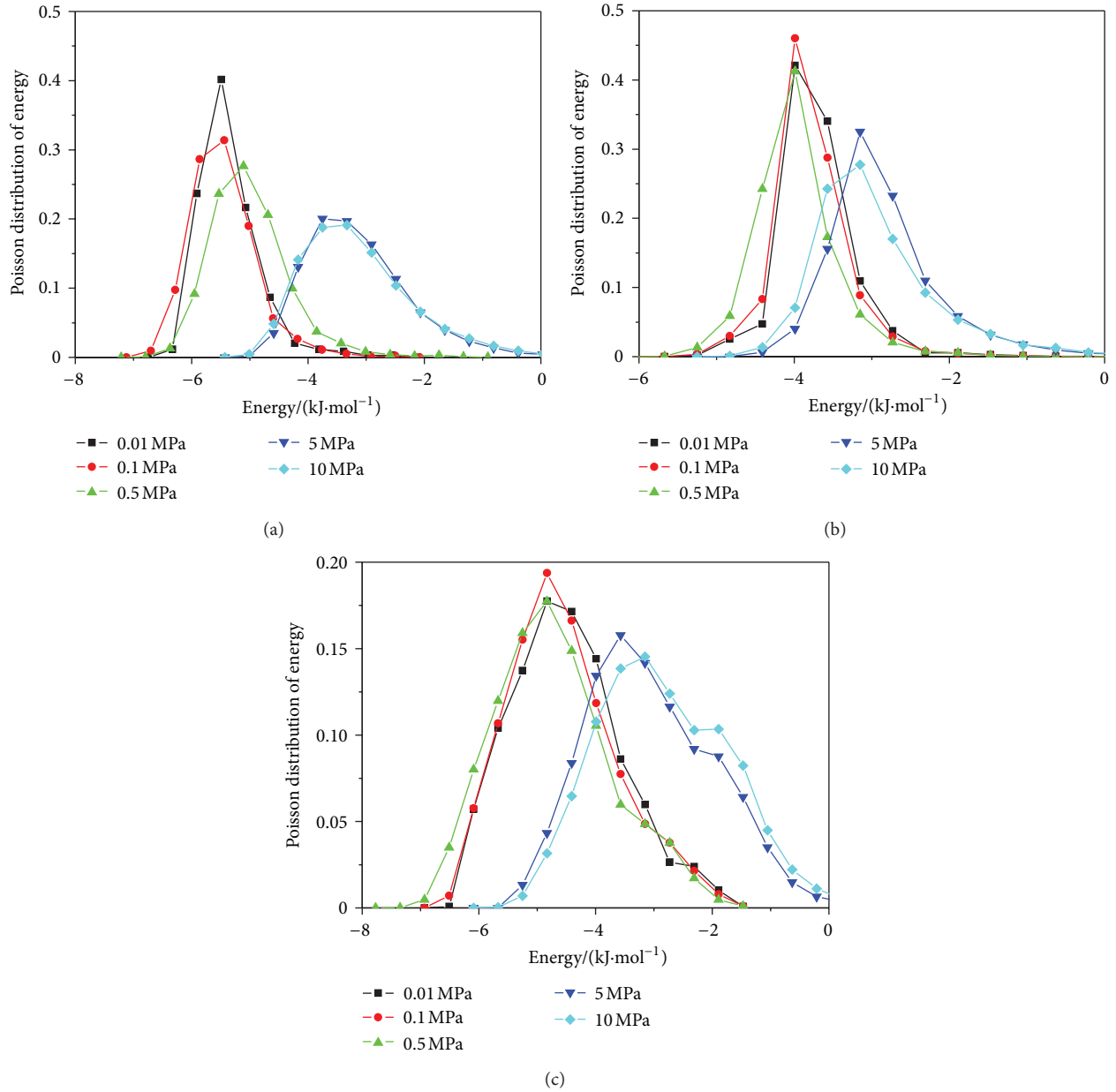

FIGURE 4: Distribution of hydrogen adsorption energy of hydrogen for (a) LiX, (b) KX, and (c) CaX at 100 K at different pressures.

number of exchangeable cations, which occupy a substantial volume, with a consequent reduction in the space available for hydrogen uptake. Maurin et al. [35] reported that the micropore volumes of Li^+, K^+, and Ca^{2+} exchanged X (Si/Al = 1.0) zeolites were 0.272, 0.204, and 0.324 mL·g^{-1}, respectively, by using nitrogen adsorption at 77 K. This may explain that larger and more cations may limit the available void volume by occupying more space themselves, which results in the lower hydrogen uptake. However, in a more confined system, adsorption may cause variation of the available void volume (due to varying sizes of pores). At low pressure, the adsorption is stronger due to the enhanced interaction of hydrogen molecules with the pore walls for the smaller pores, such as LiX and KX zeolites in this work. However, the pore volumes are small for LiX and KX zeolites. As the adsorbed amount increases, the "smaller" pores are more easily saturated or blocked. Thus, the amount adsorbed in small pores is lower at higher pressure. This usually creates a "crossover" of adsorption isotherm curves for pores of varying sizes.

We have also calculated the isosteric heat of adsorption by using the Clausius-Clapeyron equation from the isotherms at various temperatures (the hydrogen adsorption capacity is in the range of 0.02–0.7 mmol·g^{-1} at low pressure range below 1 MPa.; see Figure 1). Figure 3 illustrates the relationship between the isosteric heat of adsorption and the hydrogen adsorption capacity. The isosteric heats of adsorption of these zeolites are around 4–6 kJ·mol^{-1} indicating physisorption mechanism. As shown in Figure 3, the influence of isosteric heat of adsorption on the hydrogen uptake values is similar

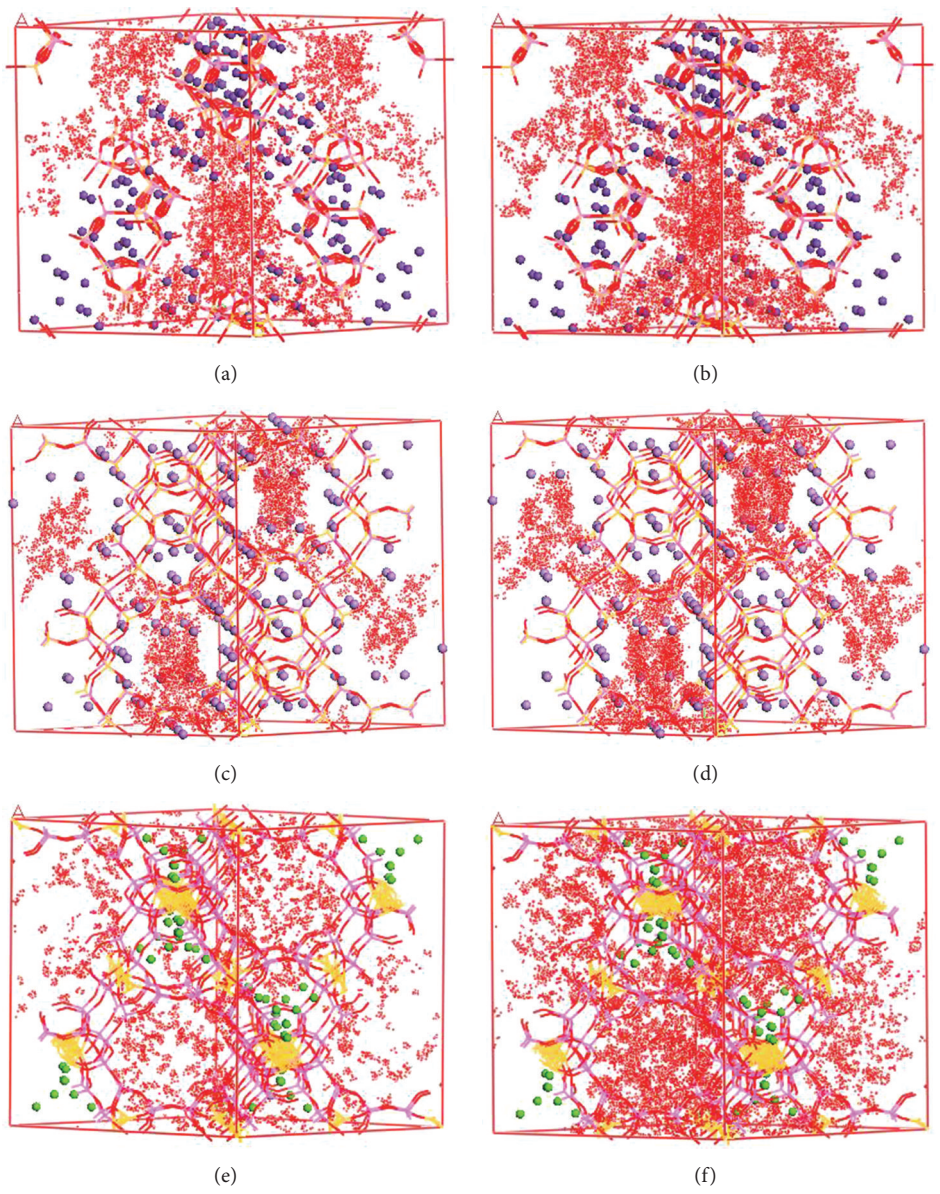

Figure 5: Mass cloud of H_2 in (a) LiX at 0.1 MPa, (b) LiX at 10 MPa, (c) KX at 0.1 MPa, (d) KX at 10 MPa, (e) CaX at 0.1 MPa, and (f) CaX at 10 MPa performed at 100 K.

for the three zeolites. Weinberger et al. [33] reported that the average heats of adsorption varied between 5.5 kJ·mol^{-1} and 7.5 kJ·mol^{-1} for the Li-LSX zeolites with different ratio of cation exchange. Li et al. [36] reported that the isosteric heats of adsorption for hydrogen on Zn^{2+} and Ni^{2+} cations exchanged X zeolites were 3.6–5.0 kJ·mol^{-1}. Moreover, for parent materials NaX, the isosteric heat of adsorption for hydrogen was in the range of 3.5–7.0 kJ·mol^{-1} [37–39]. This indicates that our calculated results are in good agreement with the experimental results reported in the literature.

As also shown in Figure 3, the isosteric heats of adsorption on all the three zeolites decrease appreciably with the increase in hydrogen adsorption capacity. This could be attributed to the energetic heterogeneities of the adsorbents [40]. For heterogeneous surfaces in the micropores of some adsorbents such as CMS and activated carbon, vertical interactions between the solid surface molecules and gas molecules decrease as the adsorption capacity increases [41]. The X and A types of zeolites are energetically heterogeneous, which could be caused by nonuniform distribution of silica-alumina in the framework, location, and distribution of one or more cations of different charge densities in the framework and presence of trace water in the cages, and so forth [40]. Moreover, the isosteric heat of adsorption for the three zeolites follows the order of LiX > CaX > KX at the same adsorbed amount (for 0.02–0.7 mmol·g^{-1}, i.e., for lower pressure range). Since isosteric heat of adsorption indicates the strength of adsorber/adsorbent interactions,

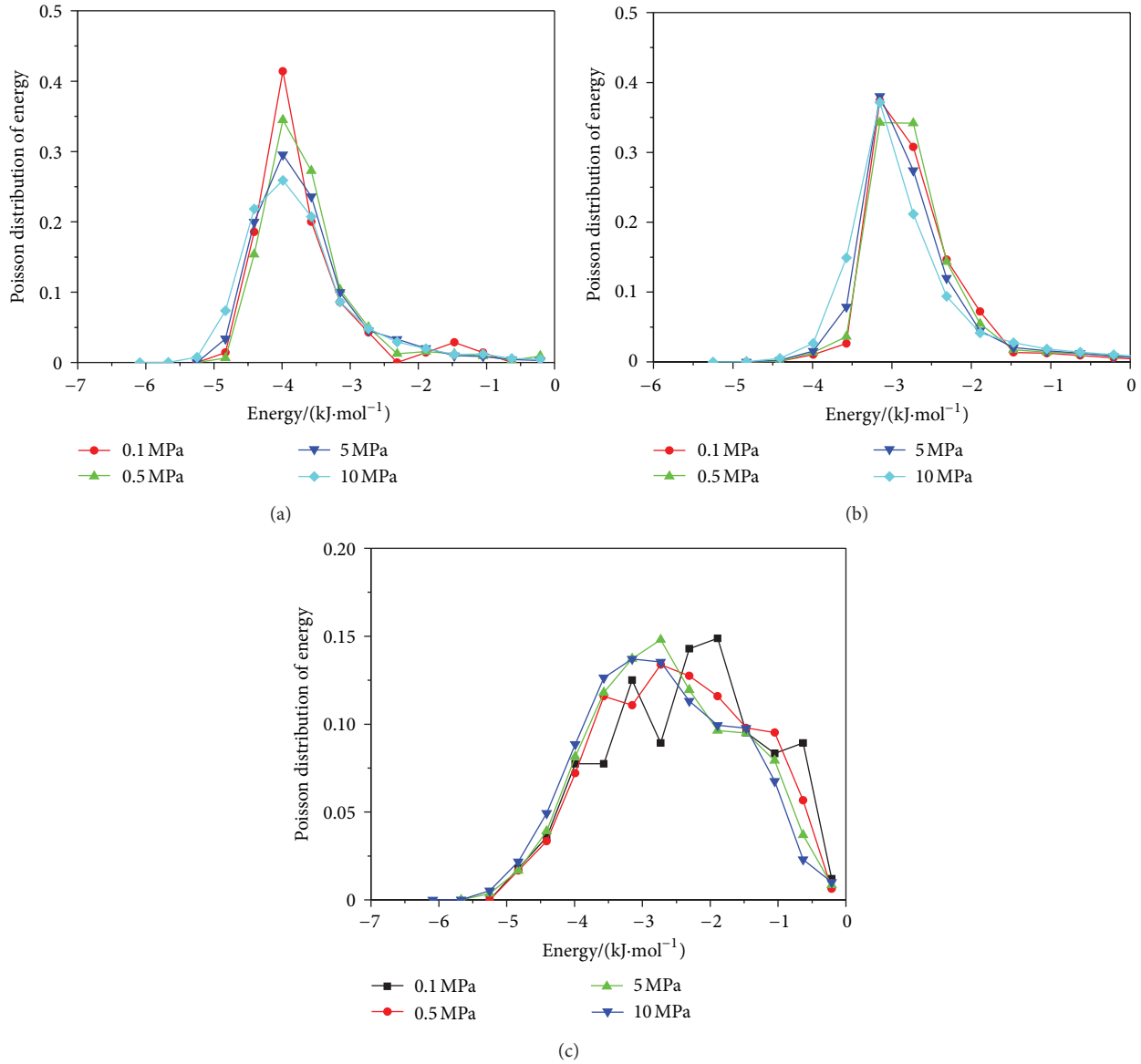

FIGURE 6: Distribution of hydrogen adsorption energy for (a) LiX, (b) KX, and (c) CaX at 293 K at different pressures.

it is illustrated that the interaction between hydrogen and zeolites pore wells (or cations) is in the order of LiX > CaX > KX at low pressure, implying that the smaller cations are able to produce a stronger electrostatic field to polarize the symmetric hydrogen molecules.

Figure 4 illustrated the distribution of hydrogen adsorption energy at 100 K and pressures P = 0.01, 0.1, 0.5, 5, and 10 MPa for LiX, KX, and CaX zeolites. For a given zeolite, only one main binding energy peak was observed and its center shifted from the high energy position to low energy position by increasing pressure. It is indicated that there are also two types of adsorption sites for hydrogen adsorption in X zeolites and the effect of the pressure (loading) on adsorption energy becomes important at 100 K. At low pressure, hydrogen molecules are adsorbed preferentially on the higher binding energy sites, such as the site II and III cations and the oxygen atoms of the framework, and these sites are relatively more quickly saturated than the lower binding energy sites, such as preadsorbed hydrogen and the inner pores of zeolite away from the surface. These were confirmed by the observation of the mass density plots as shown in Figure 5. As the pressure increases, hydrogen molecules gradually cover the lower binding sites around preadsorbed hydrogen and the inner pores of zeolite away from the surface. Eckert et al. [42] revealed that hydrogen adsorption sites in NaX zeolite were distributed near site II and III cations determined by the inelastic neutron scattering (INS) technology. Kazansky et al. [14, 15] also confirmed that the adsorption sites of hydrogen on ion-exchanged X and Y zeolites were mainly at site II and III cations inside supercages of the zeolite framework and the adjacent basic oxygen anions by using DRIFT spectra method. For the temperatures of 140 K and

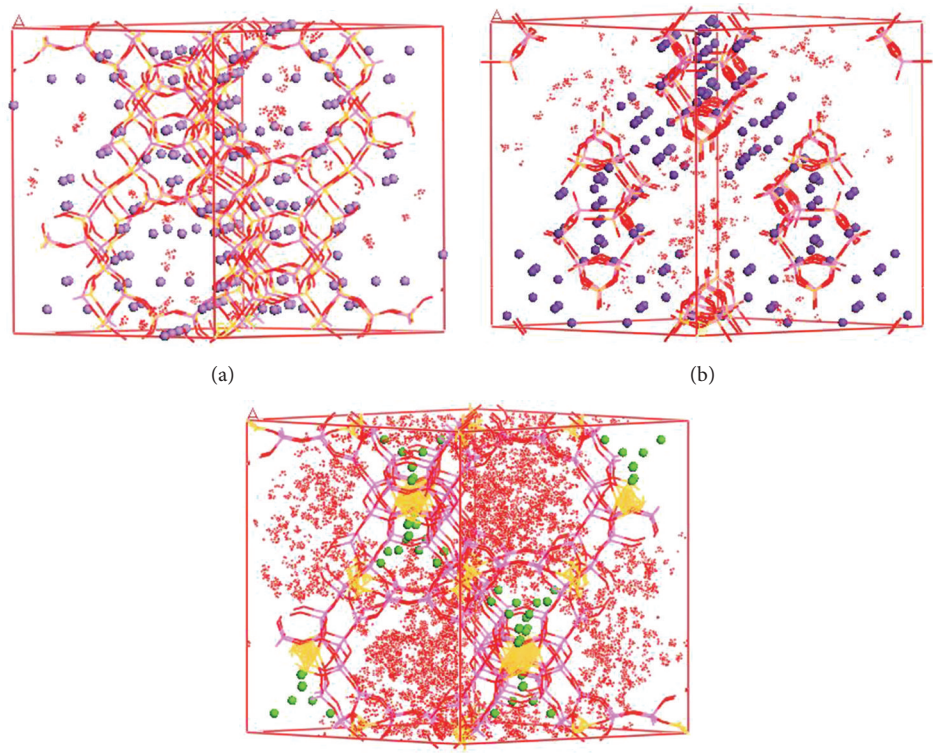

(a) (b)

(c)

Figure 7: Mass cloud of H_2 in (a) LiX, (b) KX, and (c) CaX at 293 K and 10 MPa.

195 K, the distribution of hydrogen adsorption energy at pressures P = 0.01, 0.1, 0.5, 5, and 10 MPa for LiX, KX, and CaX zeolites follows the same trend as that at 100 K.

Figure 6 shows the distribution of hydrogen adsorption energy for LiX, KX, and CaX zeolites at 293 K. At 293 K, one main binding energy peak was observed for these zeolites same as the situation at 100 K. However, the positions of these binding energy peaks are not affected by the pressure. It seems that the high binding energy sites (the extraframework metal cations) become less effective to firmly hold the hydrogen molecules at higher temperature. And the oxygen atoms of zeolite framework are the stable adsorption sites. This phenomenon was confirmed by the analysis of mass density distribution at 293 K, as shown in Figure 7. The increased temperature induces hydrogen molecules to be distributed more broadly at weak interaction sites due to the increased kinetic energy. Prasanth et al. [43] found that the physical adsorption of the cations in RhX and NiX zeolites to H_2 is negligible at 303 and 333 K, and the observed hydrogen adsorption is due to the chemisorption on nickel and rhodium metals. For the temperatures of 230 K and 260 K, the distribution of hydrogen adsorption energy at pressures P = 0.1, 0.5, 5, and 10 MPa for LiX, KX, and CaX zeolites follows the same trend as that at 293 K.

4. Conclusions

Our simulation results based on GCMC method at 100–293 K and pressures up to 10 MPa reveal that Li^+, K^+, and Ca^{2+} exchanged X zeolites are promising materials for hydrogen storage. The hydrogen adsorption is affected mainly by the type of cations exchanged in the framework structure at the same temperature and pressure. Ca^{2+} exchanged X zeolite exhibited the higher hydrogen adsorption capacity than those of Li^+ and K^+ exchanged X zeolites. This can be attributed to the larger available micropore volume, fewer Ca^{2+}, and smaller cation radius of Ca^{2+} for CaX zeolite. Upon further analysis of the simulation results, we believe that the site II and III cations and oxygen atoms of the framework are the main adsorption sites of hydrogen molecules at lower temperature, whereas the stable adsorption sites are only oxygen atoms of zeolites framework at higher temperature. Therefore, elevation of adsorption energy and increase of stable adsorption sites are the main future aspects for the design of new hydrogen storage materials by introducing the new extraframework metal cations into zeolites.

Conflict of Interests

The authors declare that there is no conflict of interests regarding the publication of this paper.

Acknowledgment

The authors gratefully acknowledge the financial support from the program for Liaoning Excellent Talents in University (LNET), China (LJQ2012016).

References

[1] L. Schlspbach and A. Zttel, "Review article Hydrogen-storage materials for mobile applications," *Nature*, vol. 414, pp. 353–358, 2001.

[2] L. Schlapbach, "Hydrogen as a fuel and its storage for mobility and transport," *MRS Bulletin*, vol. 27, no. 9, pp. 675–676, 2002.

[3] S. M. Aceves, G. D. Berry, and G. D. Rambach, "Insulated pressure vessels for hydrogen storage on vehicles," *International Journal of Hydrogen Energy*, vol. 23, no. 7, pp. 583–591, 1998.

[4] A. Dedieu, *Transitional Metal Hydrides*, Wiley-VCH, New York, NY, USA, 1992.

[5] F. Lamari Darkrim, P. Malbrunot, and G. P. Tartaglia, "Review of hydrogen storage by adsorption in carbon nanotubes," *International Journal of Hydrogen Energy*, vol. 27, no. 2, pp. 193–202, 2002.

[6] H. W. Langmi, A. Walton, M. M. Al-Mamouri et al., "Hydrogen adsorption in zeolites A, X, Y and RHO," *Journal of Alloys and Compounds*, vol. 356-357, pp. 710–715, 2003.

[7] M. G. Nijkamp, J. E. M. J. Raaymakers, A. J. van Dillen, and K. P. de Jong, "Hydrogen storage using physisorption-materials demands," *Applied Physics A*, vol. 72, no. 5, pp. 619–623, 2001.

[8] N. L. Rosi, J. Eckert, M. Eddaoudi et al., "Hydrogen storage in microporous metal-organic frameworks," *Science*, vol. 300, no. 5622, pp. 1127–1129, 2003.

[9] L. Regli, A. Zecchina, J. G. Vitillo et al., "Hydrogen storage in Chabazite zeolite frameworks," *Physical Chemistry Chemical Physics*, vol. 7, no. 17, pp. 3197–3203, 2005.

[10] F. Stéphanie-Victoire, A.-M. Goulay, and E. Cohen de Lara, "Adsorption and coadsorption of molecular hydrogen isotopes in zeolites. 1. Isotherms of H2, HD, and D2 in NaA by thermomicrogravimetry," *Langmuir*, vol. 14, no. 25, pp. 7255–7259, 1998.

[11] M. A. Makarova, V. L. Zholobenko, K. M. Al-Ghefaili, N. E. Thompson, J. Dewing, and J. Dwyer, "Brønsted acid sites in zeolites. FTIR study of molecular hydrogen as a probe for acidity testing," *Journal of the Chemical Society, Faraday Transactions*, vol. 90, no. 7, pp. 1047–1054, 1994.

[12] A. Zecchina, S. Bordiga, J. G. Vitillo et al., "Liquid hydrogen in protonic chabazite," *Journal of the American Chemical Society*, vol. 127, no. 17, pp. 6361–6366, 2005.

[13] Y. Li and R. T. Yang, "Hydrogen storage in low silica type X zeolites," *Journal of Physical Chemistry B*, vol. 110, no. 34, pp. 17175–17181, 2006.

[14] V. B. Kazansky, V. Y. Borovkov, A. Serich, and H. G. Karge, "Low temperature hydrogen adsorption on sodium forms of faujasites: barometric measurements and drift spectra," *Microporous and Mesoporous Materials*, vol. 22, no. 1–3, pp. 251–259, 1998.

[15] V. B. Kazansky, "Drift spectra of adsorbed dihydrogen as a molecular probe for alkaline metal ions in faujasites," *Journal of Molecular Catalysis A*, vol. 141, pp. 83–94, 1999.

[16] M. Feuerstein and R. F. Lobo, "Characterization of Li cations in zeolite LiX by solid-state NMR spectroscopy and neutron diffraction," *Chemistry of Materials*, vol. 10, no. 8, pp. 2197–2204, 1998.

[17] K. Seff and L. Zhu, "Cation crowding in zeolites: reinvestigation of the crystal structure of dehydrated potassium-exchanged zeolite X," *Journal of Physical Chemistry B*, vol. 104, no. 38, pp. 8946–8951, 2000.

[18] Y. I. Smolin, Y. F. Shepelev, and A. A. Anderson, "Atomic scale mechanism of CaX zeolite dehydration," *Acta Crystallographica B*, vol. 45, pp. 124–128, 1989.

[19] D. W. Lewis, A. R. Ruiz-Salvador, A. Gómez et al., "Zeolitic imidazole frameworks: structural and energetics trends compared with their zeolite analogues," *CrystEngComm*, vol. 11, no. 11, pp. 2272–2276, 2009.

[20] http://www.pwscf.org.

[21] J. R. Hill and J. Sauer, "Molecular mechanics potential for silica and zeolite catalysts based on ab initio calculations. 1. Dense and microporous silica," *Journal of Physical Chemistry*, vol. 98, no. 4, pp. 1238–1244, 1994.

[22] A. Michels, W. de Graaff, and C. A. Ten Seldam, "Virial coefficients of hydrogen and deuterium at temperatures between -175∘C and +150∘C. Conclusions from the second virial coefficient with regards to the intermolecular potential," *Physica*, vol. 26, no. 6, pp. 393–408, 1960.

[23] K. Watanabe, N. Austin, and M. R. Stapleton, "Investigation of the air separation properties of zeolites types A, X and Y by monte carlo simulations," *Molecular Simulations*, vol. 15, no. 4, pp. 197–221, 1995.

[24] E. Beerdsen, D. Dubbeldam, B. Smit, T. J. H. Vlugt, and S. Calero, "Simulating the effect of nonframework cations on the adsorption of alkanes in MFI-type zeolites," *Journal of Physical Chemistry B*, vol. 107, no. 44, pp. 12088–12096, 2003.

[25] L. Uytterhoeven, D. Dompas, and W. J. Mortier, "Theoretical investigations on the interaction of benzene with faujasite," *Journal of the Chemical Society, Faraday Transactions*, vol. 88, no. 18, pp. 2753–2760, 1992.

[26] M. P. Allen and D. J. Tildesley, *Simulation of Liquids*, Clarendon, Oxford, UK, 1987.

[27] Y. P. Joshi and D. J. Tildesley, "Molecular dynamics simulation and energy minimization of O_2 adsorbed on a graphite surface," *Surface Science*, vol. 166, no. 1, pp. 169–182, 1986.

[28] B. Weinberger, F. D. Lamari, S. B. Kayiran, A. Gicquel, and D. Levesque, "Molecular modeling of H2 purification on Na-LSX zeolite and experimental validation," *AIChE Journal*, vol. 51, no. 1, pp. 142–148, 2005.

[29] A. Gupta, S. Chempath, M. J. Sanborn, L. A. Clark, and R. Q. Snurr, "Object-oriented programming paradigms for molecular modeling," *Molecular Simulation*, vol. 29, no. 1, pp. 29–46, 2003.

[30] A. V. Kumar, H. Jobic, and S. K. Bhatia, "Quantum effects on adsorption and diffusion of hydrogen and deuterium in microporous materials," *Journal of Physical Chemistry B*, vol. 110, no. 33, pp. 16666–166671, 2006.

[31] A. W. C. van den Berg, S. T. Bromley, J. C. Wojdel, and J. C. Jansen, "Adsorption isotherms of H_2 in microporous materials with the SOD structure: a grand canonical Monte Carlo study," *Microporous and Mesoporous Materials*, vol. 87, no. 3, pp. 235–242, 2006.

[32] L. F. Wang and R. T. Yang, "Hydrogen storage properties of low-silica type X zeolites," *Industrial and Engineering Chemistry Research*, vol. 49, pp. 3634–3641, 2010.

[33] B. Weinberger, F. D. Lamari, A. Veziroglu, S. Beyaz, and M. Beauverger, "Accurate gas: zeolite interaction measurements by using high pressure gravimetric volumetric adsorption method," *International Journal of Hydrogen Energy*, vol. 34, no. 7, pp. 3191–3196, 2009.

[34] B. D. Franekel, "Zeolitic encapsulation. Part 2: percolation and trapping of inert gases in A-type zeolites," *Journal of the Chemical Society, Faraday Transactions I*, vol. 77, pp. 2041–2052, 1981.

[35] G. Maurin, P. L. Llewellyn, T. Poyet, and B. Kuchta, "Adsorption of argon and nitrogen in X-faujasites: relationships for

understanding the interactions with monovalent and divalent cations," *Microporous and Mesoporous Materials*, vol. 79, no. 1–3, pp. 53–59, 2005.

[36] J. Li, E. Wu, J. Song, F. Xiao, and C. Geng, "Cryoadsorption of hydrogen on divalent cation-exchanged X-zeolites," *International Journal of Hydrogen Energy*, vol. 34, no. 13, pp. 5458–5465, 2009.

[37] X. M. Du and E. D. Wu, "Physisorption of hydrogen in A, X and ZSM-5 types of zeolites at moderately high pressures," *Chinese Journal of Chemical Physics*, vol. 19, pp. 457–462, 2006.

[38] R. Yamk, U. Yamk, C. Heiden, and J. G. Daunt, "Adsorption isotherms and heats of adsorption of neon and hydrogen on zeolite and charcoal between 20 and 90 K," *Journal of Low Temperature Physics*, vol. 45, no. 5-6, pp. 443–455, 1981.

[39] M. A. Levin, A. A. Fomkin, A. A. Isirikyan, and V. V. Serpinskii, "Adsorption heats of hydrogen isotopes on zeolite Nax at elevated pressures," *Bulletin of the Academy of Sciences of the USSR Division of Chemical Science*, vol. 35, no. 12, p. 2594, 1986.

[40] T. C. Golden and S. Sircar, "Gas adsorption on silicalite," *Journal of Colloid And Interface Science*, vol. 162, no. 1, pp. 182–188, 1994.

[41] Y. D. Chen, R. T. Yang, and P. Uawithya, "Diffusion of oxygen, nitrogen and their mixtures in carbon molecular sieve," *AIChE Journal*, vol. 40, no. 4, pp. 577–585, 1994.

[42] J. Eckert, F. R. Trouw, and M. McMenomy, "Co-adsorption studies of hydrogen with nitrogen in zeolites," in *Proceedings of the Workshop Materials Research Using Cold Neutrons at Pulsed Neutron Sources*, August 1997.

[43] K. P. Prasanth, R. S. Pillai, H. C. Bajaj et al., "Adsorption of hydrogen in nickel and rhodium exchanged zeolite X," *International Journal of Hydrogen Energy*, vol. 33, no. 2, pp. 735–745, 2008.